Supplementary Information for

Early-onset autoimmunity associated with *SOCS1* haploinsufficiency

Hadjadj*, Castro*, et al.

*equal contribution

Contents

1. SUPPLEMENTARY NOTES

Case reports

In **family A**, the proband (A1) developed immune thrombocytopenia (ITP) at the age of 2 years. The condition was successfully treated with corticosteroids. At the age of 8, a relapse of the ITP was complicated by an intracranial hemorrhage requiring corticosteroid pulses, immunoglobulins and a thrombopoietin receptor agonist. Autoimmune hemolysis was also observed. The outcome was favorable. The patient is now aged 11, and is well controlled by mycophenolate mofetil treatment. Her mother (A2) had a history of immune thrombocytopenia at the age of 10, and also suffered from autoimmune thyroiditis and intermittent polyarthritis. Exome sequencing predicted a p.P123R heterozygous mutation in *SOCS1* in the index patient and her mother but not in the healthy father. Two of the mother's brothers were healthy with a WT *SOCS1* gene.

In **family B**, the index patient (B1) is a 6-year-old girl who presented with ITP, neutropenia, mild autoimmune hemolytic anemia, lymphadenopathy, and splenomegaly at the age of 5 years. Her medical history was unremarkable, apart from a single episode of herpes zoster at the age of 4 (after chicken pox at the age of 2). Treatment with high-dose immunoglobulins, corticosteroids, and rapamycin have controlled the cytopenia for the last 6 months. Her father (B2) developed coeliac disease at the age of 3, then suffered from moderate psoriasis and finally developed Hodgkin lymphoma at the age of 32. Trio genome sequencing predicted a heterozygous p.A9Pfs*76 mutation in *SOCS1* in the index patient and her father but not in her healthy mother. None of the 3 siblings had a history of autoimmunity, immunodeficiency or lymphoma. A 3-year-old brother (B3) suffered from severe asthma and carried the mutation, and the other tested sibling was WT.

In **family C**, the index patient (C1) presented with autoimmune hemolytic anemia and ITP at the age of 3 years. At the age of 7, she developed chronic lymphadenopathy, splenomegaly, and mild hepatomegaly. She now also suffers from mild atopic dermatitis. The autoimmune cytopenia was initially controlled with immunoglobulins and corticosteroids, although several exacerbations occurred over the years - requiring repeated corticosteroid pulses and the initiation of treatment with mycophenolate mofetil. The patient is currently 14 years old, and is clinically stable. The family's medical history is unremarkable, with no known cases of autoimmunity, immunodeficiency or lymphoma. Trio genome sequencing predicted a p.M161MAfs*46 mutation in *SOCS1* in the index patient and her asymptomatic father (C2) but not in the healthy mother.

In **family D**, the index patient (D1) is a boy diagnosed with systemic lupus erythematosus at the age of 15. His past medical history was marked by growth failure due to growth hormon deficiency from undetermined origin. He presented with a skin rash that suggested discoid lupus (**Fig. 1D**), and had a severe nephrotic syndrome. A kidney biopsy revealed class II active lupus nephritis, and laboratory tests revealed the presence of anti-nuclear antigen and anti-dsDNA autoantibodies. He was treated with corticosteroids, mycophenolate mofetil, and hydroxycholoroquine. Whole exome sequencing revealed a heterozygous p.R22W mutation in *SOCS1*. His father (D3) and a 23-year-old brother (D2) were found to be healthy carriers.

In **family E**, the index patient (E1) is a girl who presented with skin lesions suggestive of cutaneous lupus erythematosus at the age of 9. One month later, she developed polyarthritis and fever. Anti-nuclear antigen and anti-dsDNA autoantibodies were found, and

transaminases were elevated. The patient was treated with corticosteroids, hydroxychloroquine, and methotrexate but this was not effective, so cyclophosphamide was added. One year after the disease onset, the patient developed proteinuria. A kidney biopsy revealed class IV active lupus nephritis (**Fig. 1D**) requiring steroid pulses and a further course of treatment with cyclophosphamide and then with mycophenolate mofetil. She was clinically well controlled under mycophenolate mofetil but because of disabling digestive intolerance, she was switched to baricitinib (JAK1/2 inhibitor) at 2 mg once daily followed by 2 mg twice daily. Following three months of treatment, the tolerance was good while a decrease in anti-DNA autoantibodies was observed (**Supplementary Fig. 13**). Her sister (E2) was also treated for ITP diagnosed at the age of 8. She was also positive for anti-dsDNA and anti-Smith (SM) anti-ribonucleoprotein (RNP) autoantibodies. She was treated first with corticosteroids and hydroxychroloroquine, and then with immunoglobulins and rituximab. Neither of the treatments was effective, and so splenectomy was performed. During a subsequent pregnancy, the patient suffered a severe relapse of ITP; this was treated with immunoglobulins, corticosteroids, and azathioprine. The brother (E4) was suffering from moderate-to-severe plaque psoriasis since the age of 15 with intertriginous and nail psoriasis (**Fig. 1D**). He received only topical treatments. The aunt (E5) was suffering from moderate psoriasis since 44 years old, then she was diagnosed with spondyloarthritis treated by methotrexate then anti-TNFα therapy. She then developed autoimmune hepatitis and pancreatic histologically proven. Whole exome sequencing predicted a p.Y154H heterozygous mutation in *SOCS1* in the index patient. Her sister, her brother, their healthy father (E3) as well as their aunt were found to carry the mutation. Laboratory tests showed that the father had anti-SSA autoantibodies.

Supplementary three-dimensional structure analysis

P123 and Y154 are located in the SOCS1 phosphotyrosine peptide binding groove (**Fig. 1D**). In SOCS1, this groove has been shown to bind the JAK phosphorylated activation loop peptides with high affinity[5]. P123 is located at the edge of the canonical, positively charged phosphotyrosine binding site (also referred to as the pTyr (pY) pocket) formed by three β–strands (βB, βC, and βD), a loop connecting strands βB and βC, and helix αA. p.P123R mutation (at the start of strand βD) is predicted to have an impact on the pY pocket, by disturbing the network of bonds associated with the basic amino acids directly involved in phosphotyrosine binding. These include Ser125 (S125) in strand βD and Ser116 (S116) in strand βC; in the WT protein, these residues are hydrogen bonded to Arg104 (R104) in strand βB (**Fig. 1D - bottom**). Alternatively, as estimated from the comparison with the 3D structure of the SOCS3-gp130 complex (**Supplementary Fig. 3A**)[6], the long side chain of p.P123R may allow the mutated amino acid to interfere with the JAK phosphopeptide interaction near pY-2 (**Fig. 1D - bottom**).

The Y154 corresponds to a highly conserved amino acid within helix αB of the SOCS1 SH2 domain. It is part of the pTyr+3 (pY+3) hydrophobic pocket (formed between the EF and BG loops and between strand βD and helix αB) that ensures the high affinity and specificity of the phosphopeptide interaction. In the SOCS3-gp130 phosphopeptide complex, this tyrosine was shown to mediate a critical H-bond with the P+5 residue of the phosphopeptide (**Supplementary Fig. 3A**)[6]. It is noteworthy that the EF and BG loops are shorter in SOCS1 than in other members of the SOCS family. It has been proposed that this specific feature avoids a clash between the loops and the kinase domain when they bind to the JAK activation loop. p.Y154H mutation might thus also affect phosphopeptide binding at this pocket.

The p.R22W mutation is located in SOCS1's disordered N-terminal sequence, for which a 3D structure has not been experimentally determined (**Supplementary Fig. 3B**). The functional role of the N-terminal sequence on the regulation of the JAK-STAT pathway remains to be determined.

Lastly, the frameshift originating from a 4bp insertion in the SOCS1 sequence leads to a C-terminal sequence of much the same length as in the SOCS box it replaces (**Supplementary Fig. 3B**). This sequence contains five cysteine residues, and shares some features with zinc-binding domains (**Supplementary Fig. 3B**, and data not shown). An appealing hypothesis is that this novel (perhaps folded) C-terminal domain functionally replaces the SOCS box domain for binding elongin B/C.

2. SUPPLEMENTARY TABLES

Supplementary Table 1. Immunological features of patients with *SOCS1* mutations

Patients	A1 (8y)	A2 (39y)	B1 (5y)	B2 (40y)	B3 (10y)	C1 (13y)	C2 (54y)	D1 (19y)	D2 (23y)	E1 (25y)	E2 (33y)	E3 (62y)	E4 (36y)	E5 (64y)
T cells														
CD3+ (cells/mm3)	2635 (1200-2600)	1782 (807-1844)	4694 (1400-3700)	71% (55-83)	81.7% (56-84)	66% (56-84)	67% (55-83)	1105 (807-1844)	1100 (807-1844)	1296 (807-1844)	2441 (807-1844)	2965 (515-1731)	804 (521-1772)	1229 (595-1861)
CD4+ (cells/mm3)	1286 (650-1500)	934 (460-1232)	2195 (700-2200)	49.3% (51-69)	41.7% (55-62)	31% (55-62)	65% (51-69)	666 (460-1232)	710 (460-1232)	455 (460-1232)	1464 (460-1232)	1070 (286-1125)	470 (336-1126)	736 (314-1270)
CD8+ (cells/mm3)	1129 (370-1100)	804 (187-844)	2142 (190-1300)	41% (18-47)	47,5 (32%-42%)	22.4% (32-42)	31,7% (18-47)	312 (187-844)	332 (187-844)	755 (187-844)	909 (187-844)	1866 (118-786)	328 (125-780)	328 (147-836)
CD4/CD8 ratio (1.4-2.5)	1.1	1.2	1	1.2	0.9	1.4	2	2.1	2.1	0.6	1.6	0.6	1.4	2.24
CCR7+CD45RA+/CD4+ (naive)(%)	34 (58-70)	NA	43.2 (46-99)	27.6 (30-44)	55 (33-66)	44,1 (33-66)	13.2 (30-44)	65 (58-70)	48.7 (20-86)	14.8 (20-86)	44.3 (20-86)	42.7 (20-86)	37.8 (34.4-60.8)	13.2 (23.4-62.7)
CD31+CD45RA+/CD4+ (recent naive thymic emigrant) (%)	17 (43-55)	NA	NA	NA	NA	NA	NA	43.7 (43-55)	33 (30-48)	12.2 (30-48)	35.2 (30-48)	12.4 (20-28)	NA	NA
CD45RO+/CD4+ (memory) (%)	66	NA	26	67	38.6	54	80.8	35	51.3	85.2	55.7	57.3	53	86
CCR7+CD45RA+/CD8+ (naive) (%)	76 (52-68)	NA	38,5 (16-100)	NA	NA	12 (20-95)	NA	60.3 (52-68)	53.8 (37-50)	20.7 (37-50)	49.4 (37-50)	4.9 (29-57)	45.3 (35.3-68.3)	8.2 (10.5-31.7)
CCR7+CD45RA−/CD8+ (central memory) (%)	2.5 (3-4)	NA	NA	NA	NA	0.26 (3-4)	NA	10.8 (3-4)	5.9 (6-16)	3.7 (6-16)	6.2 (6-16)	2.3 (3-14)	28.9 (19.7-33.1)	11.6 (4.6-14.2)
CCR7−CD45RA−/CD8+ (effector memory) (%)	11.5 (11-20)	NA	NA	NA	NA	9.76 (11-20)	NA	17.8 (11-20)	26.7 (25-37)	53.7 (25-37)	23.9 (25-37)	22 (20-41)	33.9 (9.1-25.7)	25.7 (22-38.5)
CCR7-CD45RA+/CD8+ (exhausted effector memory, EMRA) (%)	10 (16-28)	NA	NA	NA	NA	77.8 (16-28)	NA	11.1 (16-28)	13.5 (8-20)	21.9 (8-20)	20.5 (8-20)	70.8 (11-26)	<1 (1.2-8.8)	54.5 (21.3-55)
NK cells														
CD16+CD56+ (cells/mm3)	125 (100-480)	261 (89-362)	363 (130-720)	NA	NA	NA	NA	146 (89-362)	163 (89-362)	69 (89-362)	1056 (89-362)	236 (62-565)	102 (70-523)	196 (77-321)
CD16+CD56+ (%)	4 (4-17)	12 (5-20)	6 (4-17)	8.9 (7-31)	9.7 (3-22)	2.2 (3-22)	21.3 (7-31)	9.2 (5-20)	11 (5-20)	4.6 (5-20)	29 (5-20)	7.2 (5-33)	10 (5-33)	11 (3-23)

Supplementary Table 1. Immunological features of patients with *SOCS1* mutations (continued)

CD19+ (cells/mm3)	376 (273-860)	**130** (169-372)	1124 (370-1400)	NA	NA	NA	NA	319 (133-255)	209 (133-255)	**121** (133-255)	**85** (169-271)	**86** (169-271)	98 (67-516)	227 (107-271)
CD19+ (%)	12 (6.1-25.2)	**6** (7.2-11.2)	18 (14-33)	7 (4.8-22.7)	**3.8** (7-24)	**29,7** (6.5-24)	**3.9** (4.8-22.7)	20.19 (6.6-10.8)	12.1 (6.6-10.8)	6.9 (6.6-10.8)	**2.7** (7.2-11.2)	**2.6** (7.2-11.2)	9.2 (4.4-19.4)	13.5 (6.8-21.1)
CD27- IgD+/CD19+ (naive) (%)	**93** (59.7-88.4)	63 (58-72.1)	**81.8** (70-80)	67.6 (36.4-84)	68.2 (49-100)	68,7 (61.6-87.4)	68.8 (36.4-84)	**93.4** (65.6-79.6)	**93.4** (65.6-79.6)	**88.3** (65.6-79.6)	**72.7** (58-72.1)	65.4 (58-72.1)	37.4 (35.5-64.5)	**85.8** (35.5-64.5)
CD27+ IgD+/CD19+ (marginal zone) (%)	4 (3.1-18)	**9** (13.4-21.4)	**14** (7-12)	11.1 (3.1-20.8)	12.1 (2-28)	5.4 (2.6-13.4)	7.7 (3.1-20.8)	**1.8** (7.4-13.9)	**4.1** (7.4-13.9)	**1** (7.4-13.9)	**11.7** (13.4-21.4)	**8.8** (13.4-21.4)	16.5 (15.7-35.2)	**7.4** (15.7-35.2)
CD27+ IgD-/CD19+ (switched memory) (%)	**0.7** (2.9-17.4)	17 (9.2-18.9)	**1.9** (5-12)	8.2 (5.1-31.8)	7.6 (1-43)	**2.9** (4-21.2)	**4.9** (5.1-31.8)	**2.4** (7.2-12.7)	**1.3** (7.2-12.3)	**6** (7.2-12.3)	10.7 (9.2-18.9)	14.1 (9.2-18.9)	35.4 (10.2-32.3)	**4** (10.2-32.3)
CD21lowCD38low (autoreactive) (%) (<5%)	**16**	**5.5**	**20.2**	**5.6**	**5.32**	**8.68**	3.7	4.9	1.2	**5.9**	**12.2**	**8.3**	NA	NA
CD24++ CD38++/CD19+ (transitional) (%) (<10%)	2.6	2.1	4	5.9	4.3	**10.21**	**13.4**	**20.8**	9	**47.2**	6.6	1.2	0.6	9.1
CD24- CD38++/CD19+ (plasmablasts) (%) (<5%)	0.2	0.6	NA	2.2	1.1	0.2	0.9	0.4	0.3	0.4	0.4	0.2	NA	NA
BAFF serum levels (pg/ml) (<1078)	**2521**	**1935**	680	674	NA	**1164**	974	**1312**	710	**1182**	882	884	NA	NA
Autoantibodies	Coombs +	ANA Anti-thyroperoxydase Anti-mitochondrial M2 Anti-GP210	Coombs +	NA	NA	Coombs +	NA	ANA Anti-DNA Anti-SSA/Anti-SSB	No	ANA Anti-DNA Anti-U1-RNP	ANA Anti-DNA	ANA anti-SSA	No	ANA Anti-SCL

Lymphocyte reference values as a function of the age in brackets and were established by the laboratory on a pool of controls. Values above the reference range are marked in red and below in blue. ANA, antinuclear antibody; ISG, interferon type I gene signature; NA, not available.

Supplementary Table 2. Antibodies used for flow cytometry

Antibody	Source	Clone
anti-CD45-PerCP-Cy5.5	Beckton Dickinson	2D1 (HLe-1)
anti-CD3-FITC	Beckton Dickinson	SK7
anti-CD4-PE-Cy7	Beckton Dickinson	SK3
anti-CD8-APC-Cy7	Beckton Dickinson	SK1
anti-CD19-APC	Beckton Dickinson	SJ25C1
anti-CD16-PE	Beckton Dickinson	B73.1
anti-CD56-PE	Beckton Dickinson	NCAM16.2
anti-CD4-PerCP-Cy5.5	Beckton Dickinson	SK3
anti-CD8-APC-H7	Beckton Dickinson	SK1
anti-CD45RA-FITC	Beckton Dickinson	L48
anti-CD45RO-PE	Beckton Dickinson	UCHL1
anti-CCR7-PE-Cy7	Beckton Dickinson	3D12
anti-CD31-AF647	Beckton Dickinson	M89D3
anti-CD19-V500	Beckton Dickinson	HIB19
anti-CD27-V450	Beckton Dickinson	M-T271
anti-CD24-FITC	Beckton Dickinson	ML5
anti-IgD-PE	Beckton Dickinson	IA6-2
anti-CD38-PE-Cy7	Beckton Dickinson	HIT2
anti-CD21-APC	Beckton Dickinson	B-ly4
anti-CD14-FITC	Beckman Coulter	RMO52
anti-CD14- APC	BD Pharmingen	M5E2
anti-CD3-PerCP	BD Pharmingen	SK7
anti-CD45RO PE-CF 594	Beckton Dickinson	UCHL1
anti-CD4 PE-Cy7	Beckman Coulter	SFCI 12T4D11
anti-TNF-a-PE	BD Pharmingen	MAb11
anti-IL4-APC	eBioscience	17-7049-42
anti-IFNg-FITC	BD Bioscience	B27
anti-IL17A-PE	Invitrogen	12-7179-42
anti-CTLA4-PE	BD Pharmingen	BNI3
anti-CD25-PE-Cy7	BD Pharmingen	M-A251
anti-Foxp3-APC	Invitrogen	PCH101
anti-Helios-eF450	Invitrogen	22F6
anti-P-STAT1-AF647	BD phosflow	4a
anti-CD11c PE Cy5	BD Bioscience	BU.15
anti-CD14 VioBlue	Beckman Coulter	TUK4
anti-CD16 BV510	Sony	3G8
anti-CD33-PerCP-Cy5.5	Beckton Dickinson	P.67.6
anti-pSTAT1-BV421(pY701)	Beckton Dickinson	4a

Supplementary Table 3. Primer used for sequencing and real-time quantitative RT-PCR

Name	Sequence
p.P123R mutagenesis	GCCTCGGGACgCACGAGCATC
	CATCTTCACGCTAAGGGCG
p.A9fs76 mutagenesis	GCCGACAATGCAGTCTCC
	GCCACCTGGTTGTGTGCT
p.M161fs*46 mutagenesis	gccgcATGCTGGGGGCCCCGCTGCG
	GCGGCGCGGCGCCGCCAC
p.R22W mutagenesis	GCCCCGACGGtGGCCAGAACC
	TCTGCTGCTGTGGAGACTGCATTGTC
p.Y154H mutagenesis	GCTGGAGCACcACGTGGCGGC
	AGCTCGAAGAGGCAGTCGAAG
SOCS1 genomic DNA 1	GCTGGCCCCTTCTGTAGGAT
	AGCTCGAAGAGGCAGTCGAA
SOCS1 genomic DNA 2	CCGATTACCGGCGCATCA
	GGAACTGCTTTTTCGCCCTTAG
SOCS1 cDNA 1	GACGCCTGCGGATTCTACTG
	ACGGTGGCCACGATGC
SOCS1 cDNA 2	GCTGCACGGCTCCTG
	AGAGGTAGGAGGTGCGAGTT
SOCS1 cDNA 3	CCTTAGCGTGAAGATGGCCT
	GAACGGAATCTGCGGAAGTG
CXCL10 QPCR	TTCAAGGAGTACCTCTCTCTAG
	CTGGATTCAGACATCTCTTCTC
CXCL9 QPCR	Performed in Taqman, sequence not avalaible
CISH QPCR	AAAACTGGTGCAGCCCTTTGTA
	GCCACCAGACGGTTGATGAC
PIM1 QPCR	CGGGAAGCTGGAGACAGAAG
	CCCAGCAAATAGCAGCCTTT

QPCR, real-time quantitative RT-PCR

3. SUPPLEMENTARY FIGURES

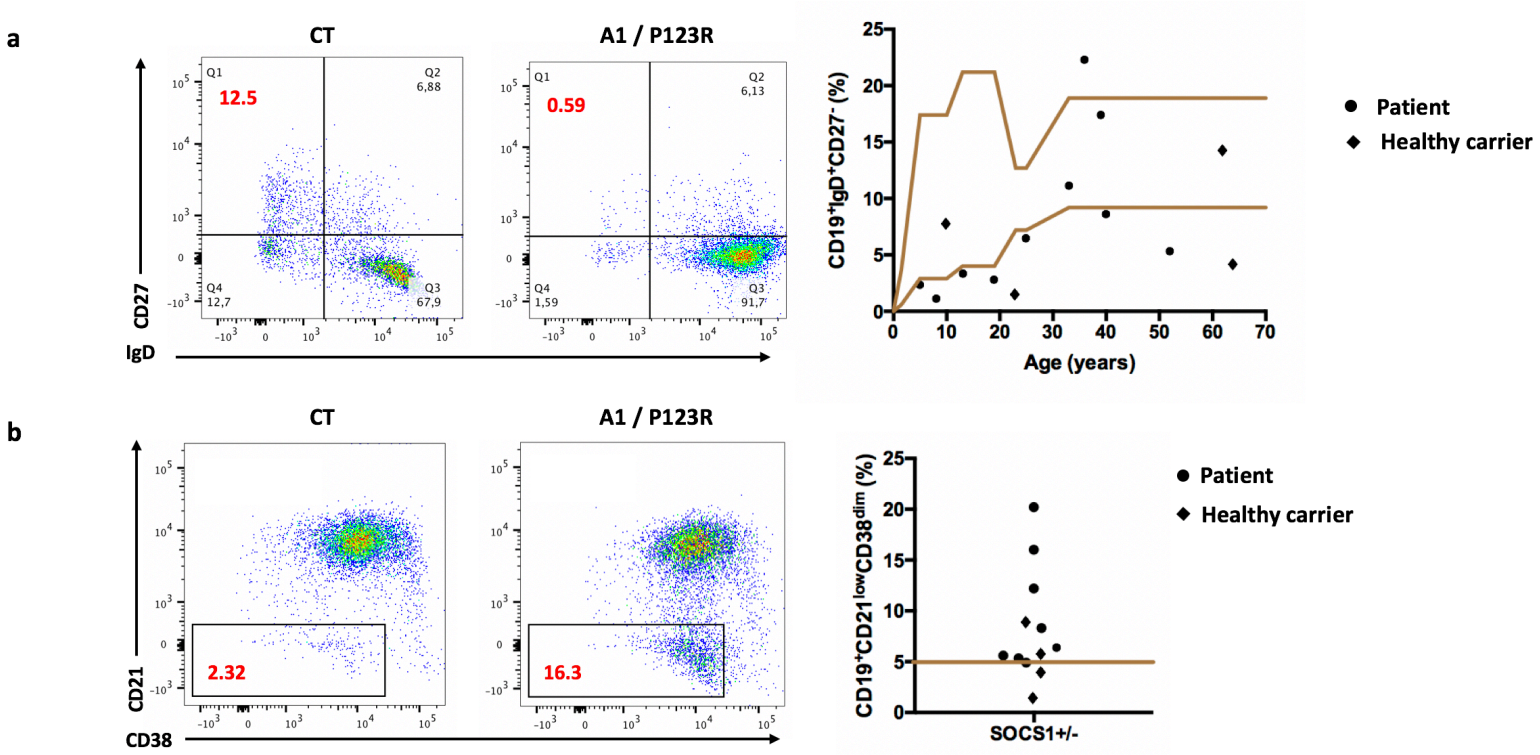

Supplementary Figure 1. B-cell phenotype

(**A**) Left: a representative flow cytometry analysis of CD27 and IgD markers in $CD19^+$ B cells from an HC and from patient A1 (p.P123R mutation). Right: $CD19^+CD27^-$ IgD^+ B cells (as a percentage of total $CD19^+$ B cells) in the peripheral blood of *SOCS1* mutation carriers (n=13). Normal range from the laboratory are between the brown lines. (**B**) Left: a representative flow cytometry analysis of CD21 and CD38 markers in $CD19^+$ B cells from an HC and from patient A1 (p.P123R mutation). Right: $CD19^+CD21^{low}$ $CD38^{dim}$ B cells (as a percentage of total $CD19^+$ B cells) in the peripheral blood of *SOCS1* mutation carriers (n=13). Normal range from the laboratory is below the brown line (5%).

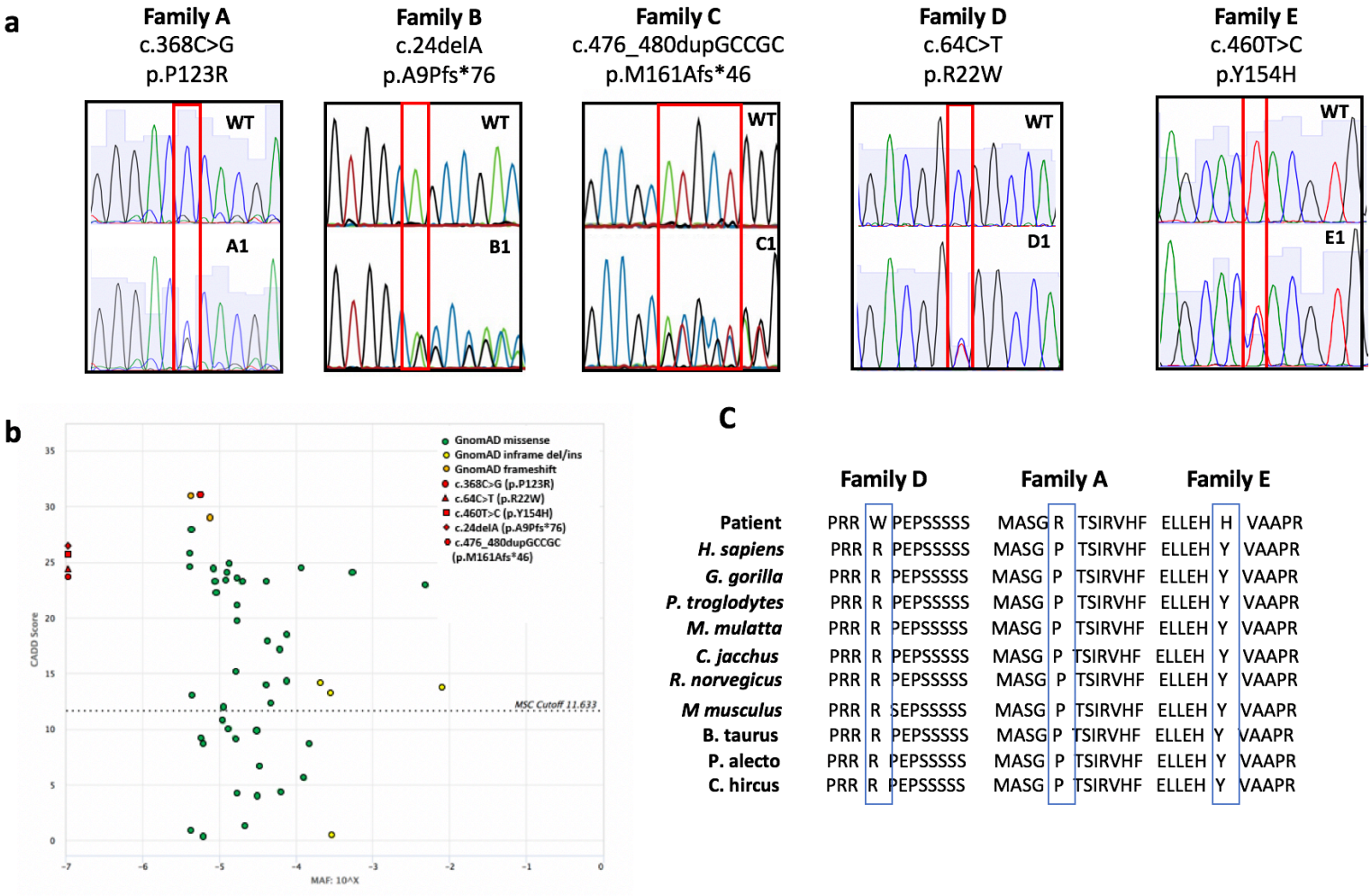

Supplementary Figure 2. Sanger sequencing and *in silico* analysis

(A) Sanger sequencing fluorograms showing five genomic *SOCS1* mutations identified in five families. **(B)** The predicted Combined Annotation Dependent Depletion (CADD) scores and general minor allele frequency (MAF) for the mutations found in patients (red) and mutations reported in the GnomAD database (missense, green; deletion/insertion, yellow; frameshift, orange). The CADD mutation signification cut-off score [99% confidence interval] for *SOCS1* is indicated by a dashed line[1]. **(C)** Protein sequence alignment for SOCS1 from various vertebrate species. Conserved amino acids affected by mutations are highlighted in blue.

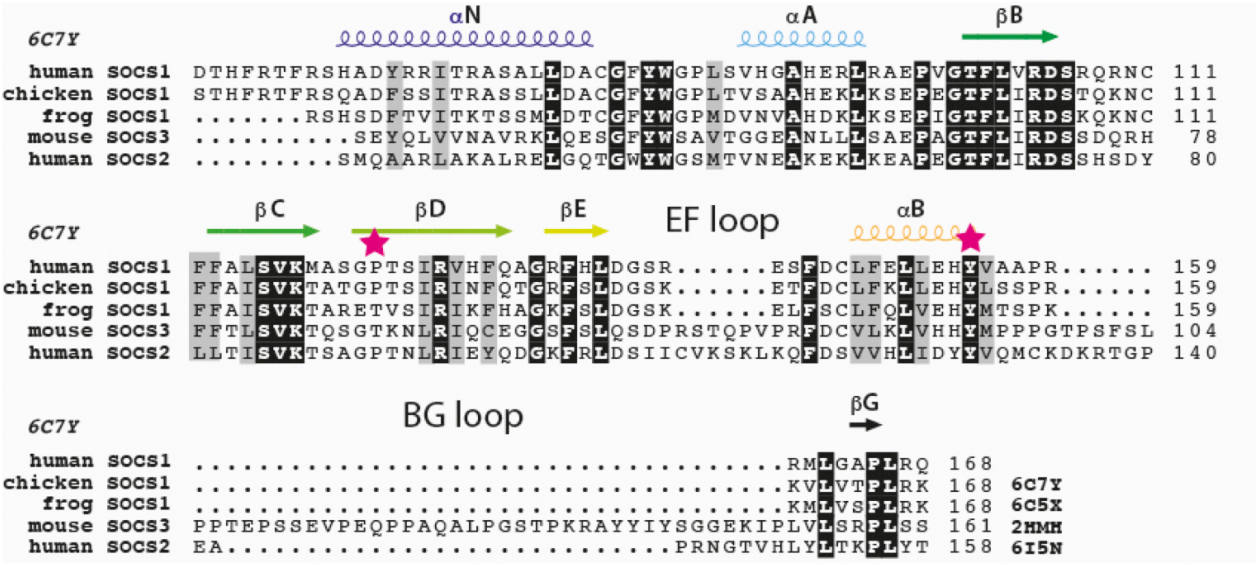

Supplementary Figure 3. Alignment of SOCS protein sequences.

Alignment of the sequences of human SOCS1 sequences with those of SOCS sequence with experimentally solved 3D structures. Protein data bank identifiers are indicated at the end of the sequences, with the observed secondary structures of chicken SOCS1 (Protein Data Bank 6C7Y) taken as a reference on top of the alignment. Identical amino acids are shown white on a black background, positions where hydrophobicity is conserved are shown grey. Mutated amino acids are highlighted with a star.

a **b**

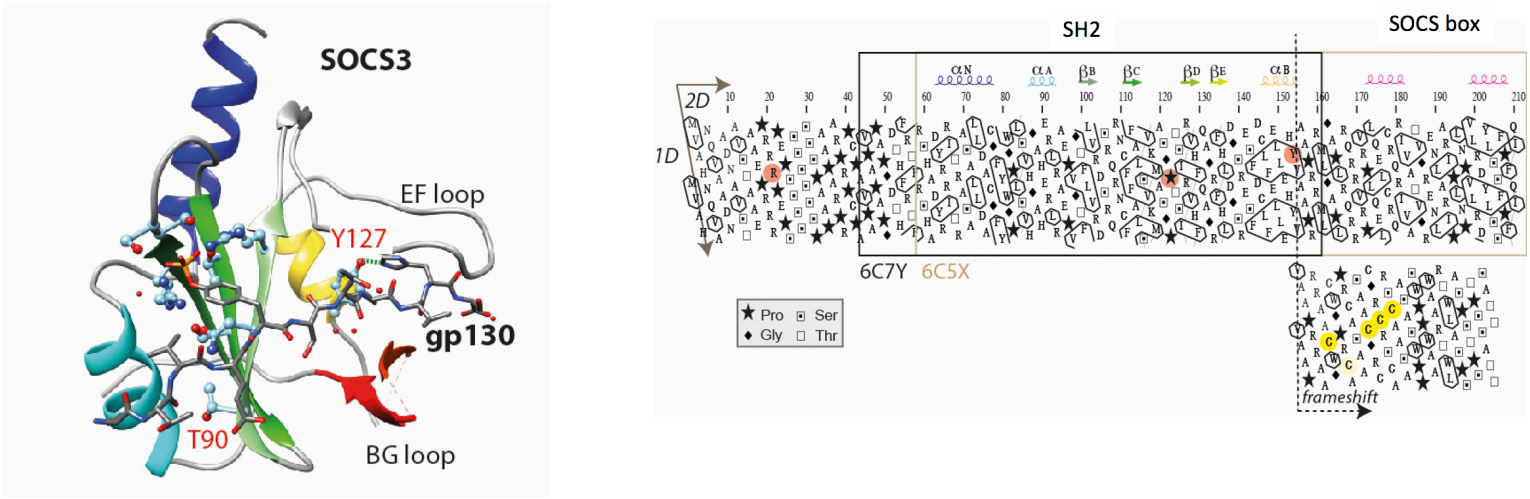

Supplementary Figure 4. Structural analysis

(A) Experimental 3D structure of the SOCS3-gp130 complex (Protein Data Bank 2HMH), highlighting the position of the phosphopeptide within the binding groove. **(B)** Two-dimensional representation of the human SOCS1 protein sequence, derived from hydrophobic cluster analysis (Bitard-Feildel et al, 2018). The sequence is written on a duplicated α-helical net, and the clusters formed by strong hydrophobic amino acids are highlighted; these clusters mainly correspond to the internal faces of regular secondary structures. A high density of hydrophobic clusters (as observed for the SH2 domain and the SOCS box, for which the observed secondary structures are indicated at the top of the plot) indicates the presence of foldable domains. Regions devoid of long hydrophobic clusters are either disordered (as is the case for the N-terminal region) or require ions to fold (as is perhaps the case for the C-terminal region in the mutated SOCS1 protein, where a frameshift affects cysteine residues that might bind zinc ions). Mutated amino acid residues are indicated by an asterisk.

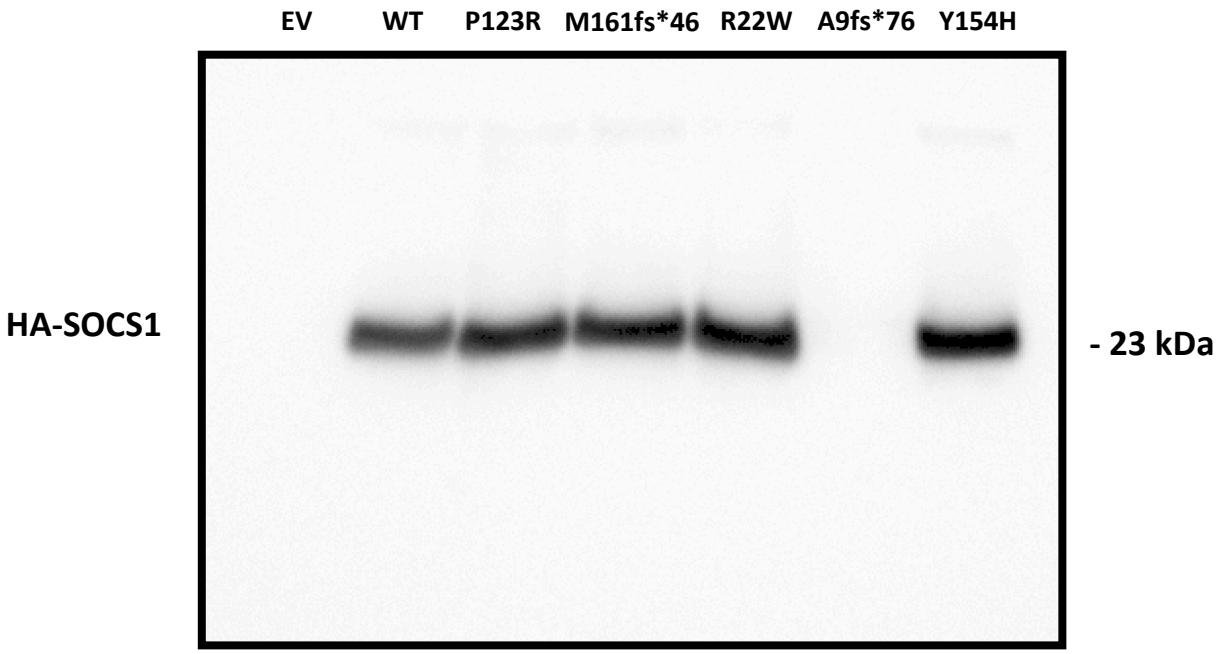

Supplementary Figure 5. Full western-blot of SOCS1 protein expression in transfected cells. HEK293T cells were transiently transfected with an empty vector (EV), a vector coding for hemagglutinin (HA)-tagged wild type (WT) SOCS1, or vectors coding for the five HA-tagged mutant SOCS1 proteins. Lysates were incubated with anti-HA antibodies. Data are representative of two independent experiments.

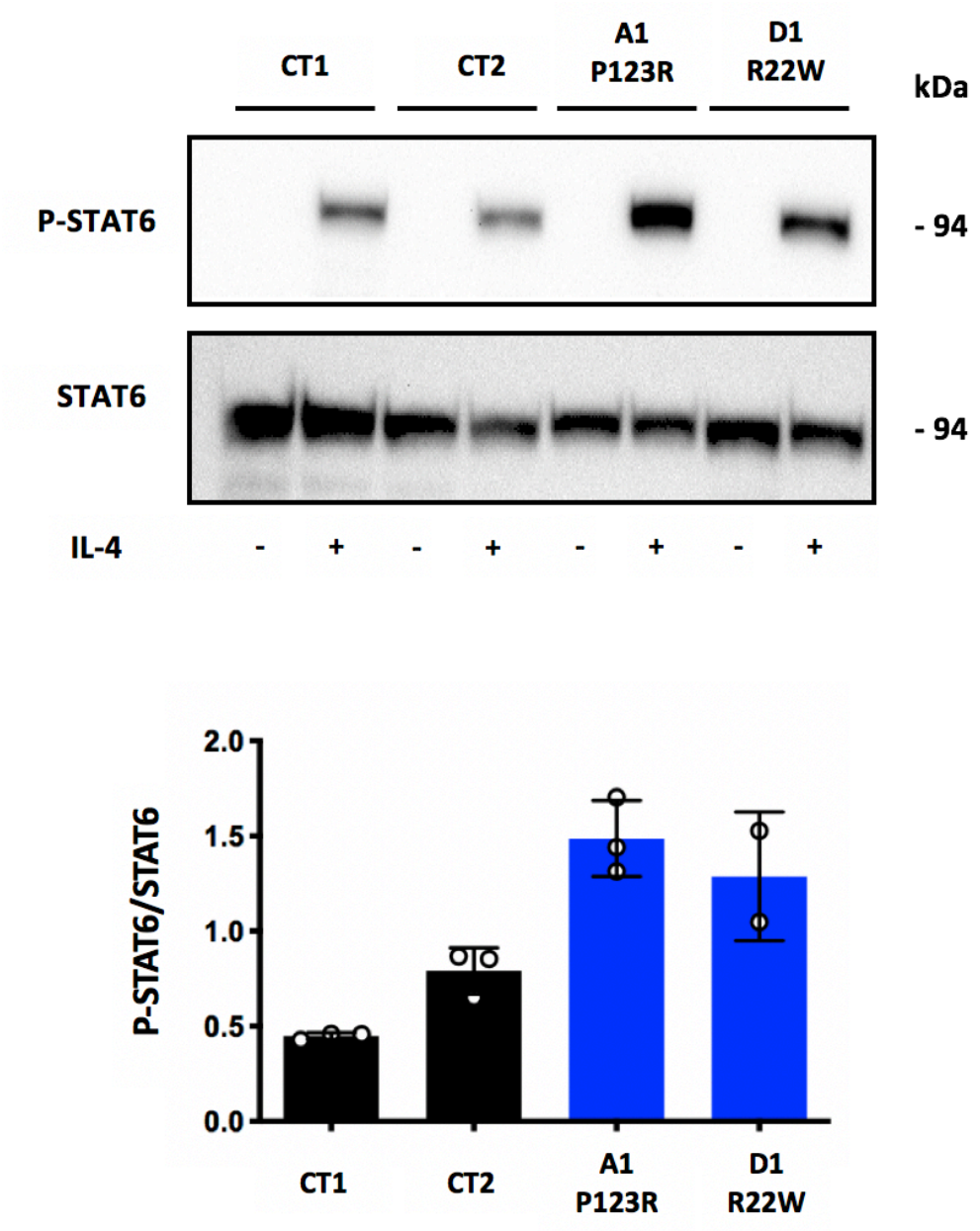

Supplementary Figure 6. Increased IL-4 mediated-STAT6 phosphorylation

Top: Western blot of EBV-B cells from healthy controls (CT) and from patient A1 (p.P123R mutation) and D1 (p.R22W mutation) after stimulation with IL-4 (10ng/ml for 1h). Lysates were incubated with the anti-P-STAT6 and anti-STAT6 antibodies. Bottom: densitometric quantification of the phospho-STAT6/total STAT6 ratio upon stimulation with IL-4. Data indicate mean with SD and are representative of n=3 (A1) and n=2 (D1) independent experiments.

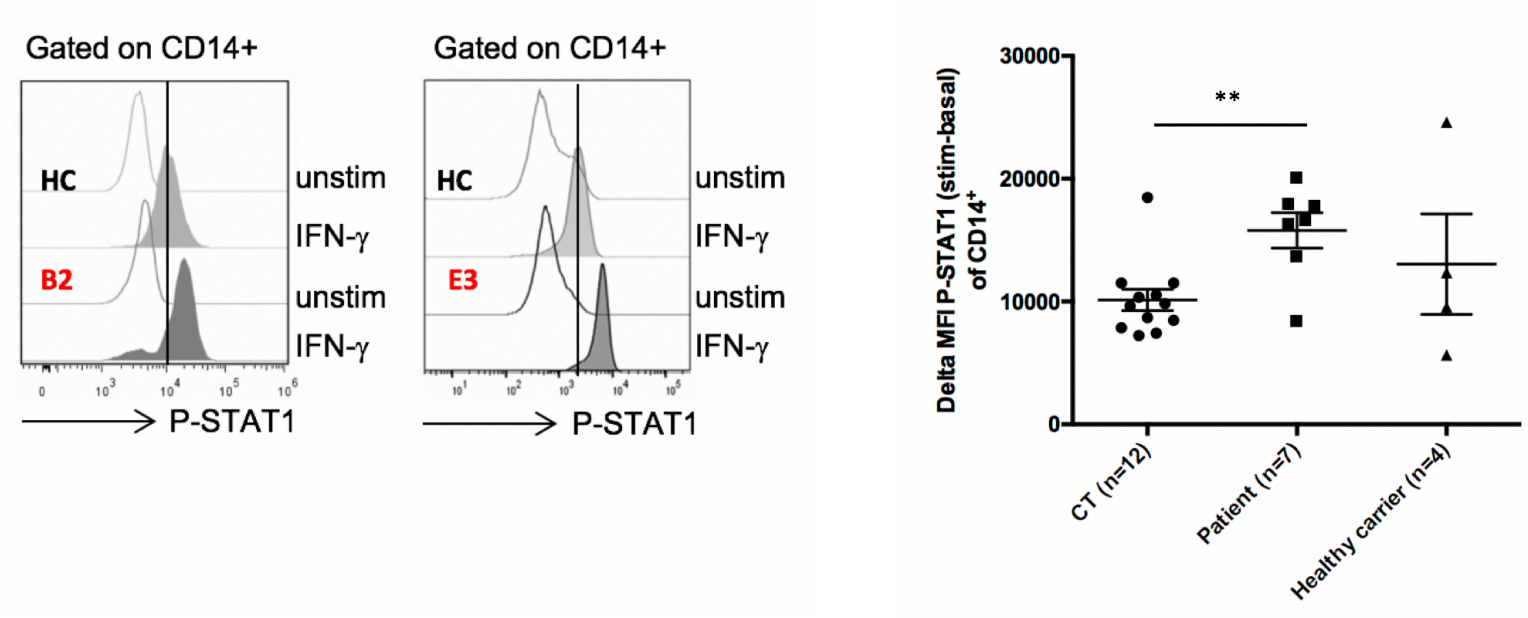

Supplementary Figure 7. STAT1 phosphorylation in response to IFN-γ in primary monocytes

Primary monocytes ($CD3^-CD19^-CD14^+$) from healthy controls (CT), patients and healthy carriers were stimulated with IFN-γ for 15 min and STAT1 phosphorylation (P-STAT1) was determined by intracelular flow cytometry. Left: Representative histograms showing P-STAT1 at baseline (unstim, open line) and after stimulation (IFN-γ, filled line) from patient B2 (p.A9fs*76 mutation) and healthy carrier E3 (p.Y154H mutation) . Right: Delta in P-STAT1 MFI before and after IFN-γ stimulation pooled from CT (n=11), patients (n=7) and healthy carriers (n=4). Data indicate mean with SEM. Two-tailed p value was calculated with unpaired t test ($p = 0.0022$). **$P \leq 0.01$.

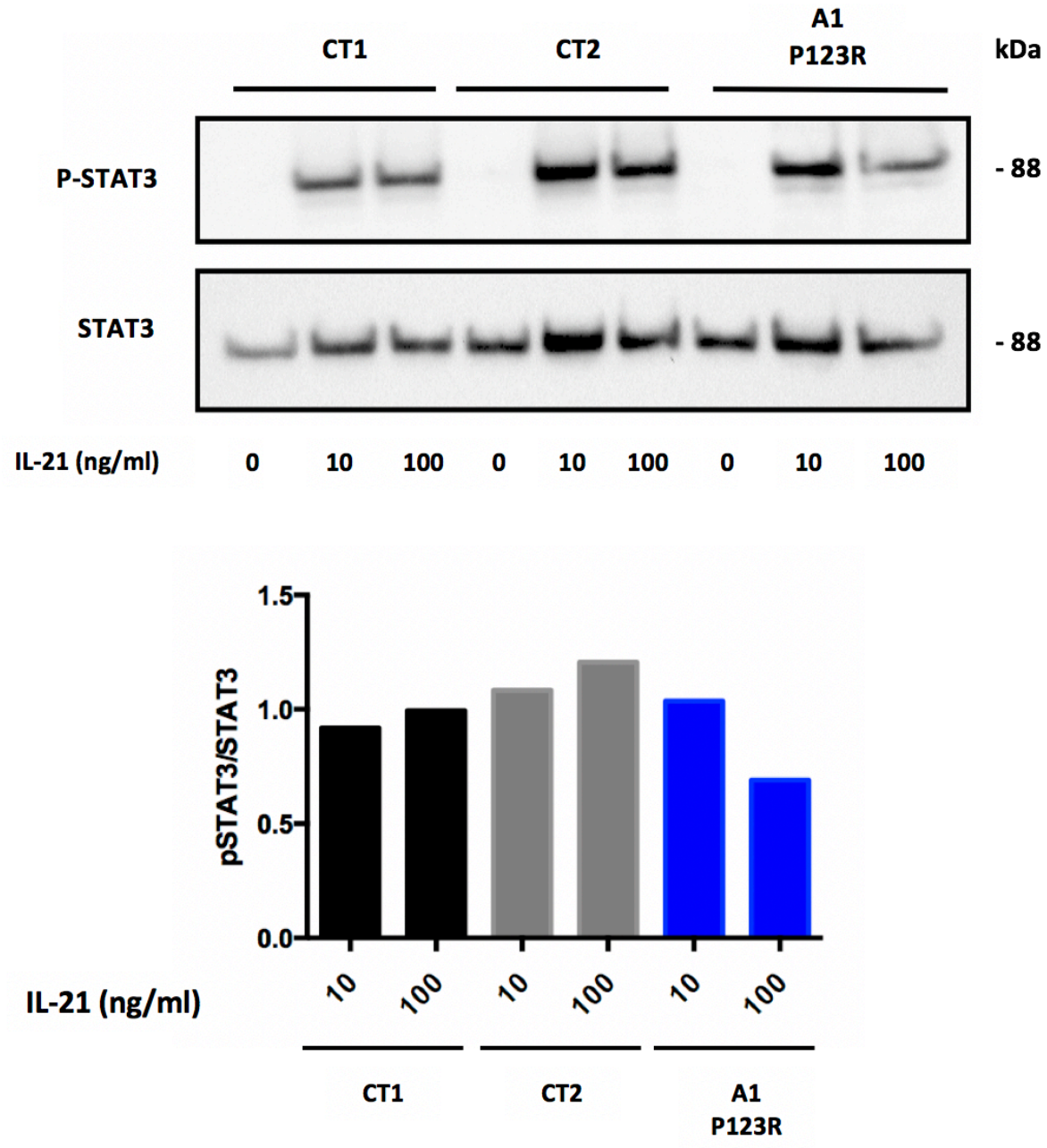

Supplementary Figure 8. No evidence of increased IL-21 mediated STAT3 phosphorylation

Top: Western blot of EBV-B cells from CT and from patient A1 (p.P123R mutation) after stimulation with IL-21 for 1h at the indicated concentrations. Lysates were incubated with the indicated anti-P-STAT3 and anti-STAT3 antibodies. Bottom: densitometric quantification of the phospho-STAT3/total STAT3 ratio upon stimulation with IL-21. Experiment performed once.

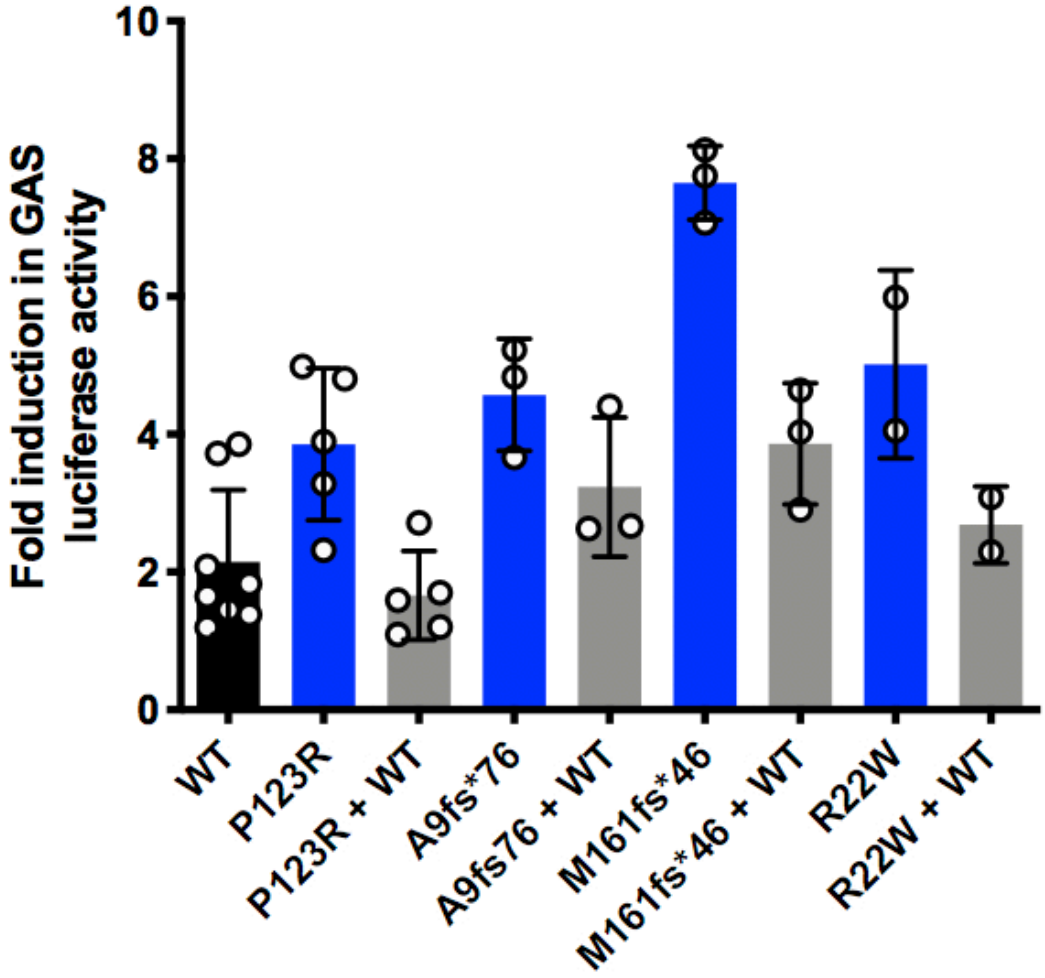

Supplementary Figure 9. No evidence of dominant-negative effect of SOCS1 mutants

HEK293T cells were transiently cotransfected with a gamma-activated sequence-driven IFN-γ reporter plasmid (GAS), a *Renilla* luciferase control vector, WT SOCS1 or/and mutant plasmids, and then stimulated with IFN-γ for 24 hours. The response to IFN-γ was evaluated by assaying the firefly luciferase activity (normalized against *Renilla* luciferase activity to compensate for differences in transfection efficiency). The results correspond to the fold-difference between the stimulated state and the unstimulated state. Data indicate mean with SD of n=2 (R22W), n=3 (A9fs*76 and M161fs*46) and n=5 (P123R) independent experiments.

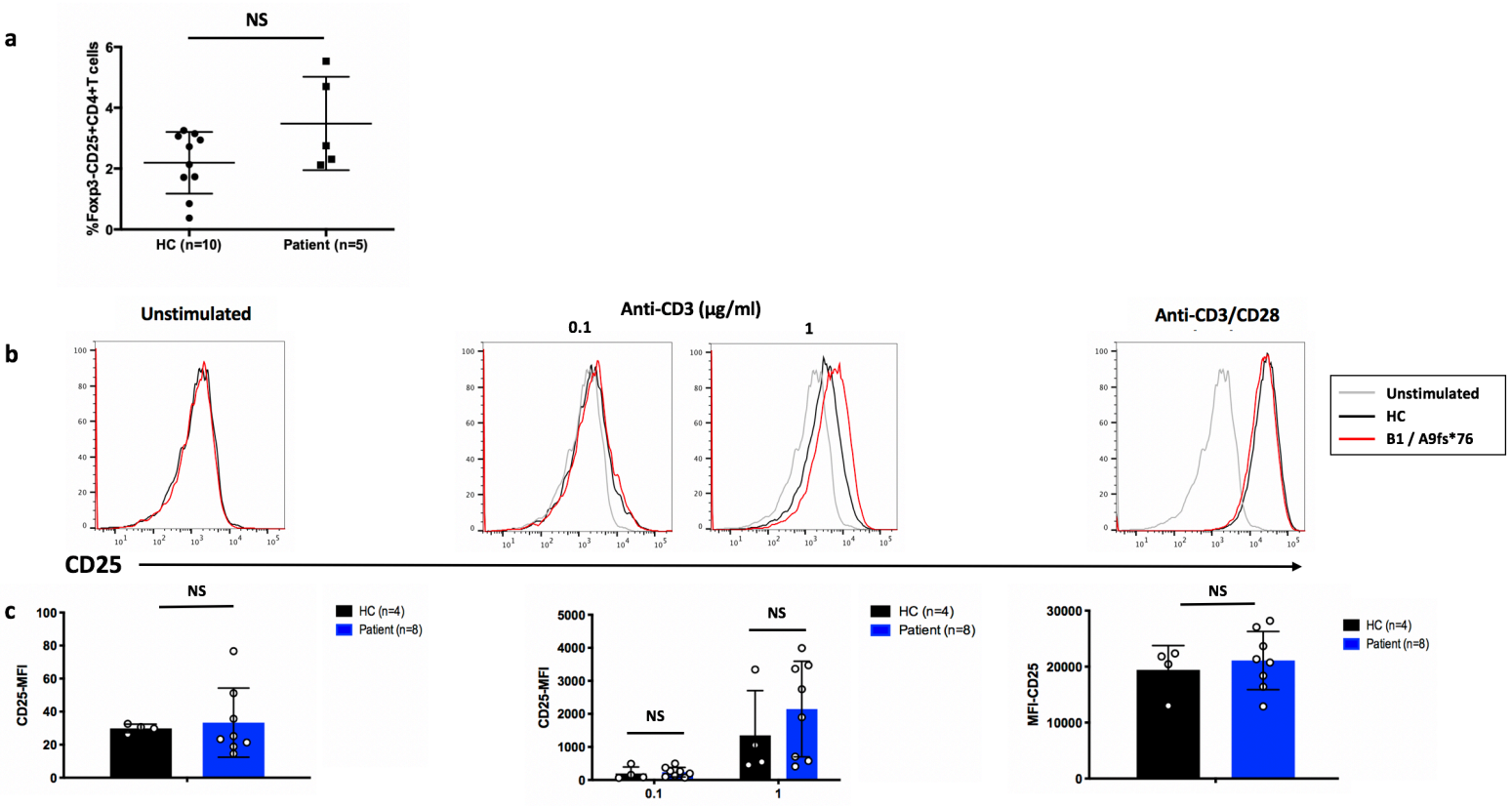

Supplementary Figure 10. CD25 expression on T cells

(A) $CD25^+$ $FoxP3^-CD4^+$ T cells (as a percentage of total $CD4^+$ T cells) in the peripheral blood of HCs (n=10) and patients (n=5). **(B)** Representative flow cytometry histograms of CD25 expression on T-cell blasts ($CD3^+$) at day 10 of culture from healthy controls (HC) and from patient B1 (p.A9fs*76 mutation) in a steady state or after 4 days of stimulation with anti-CD3 antibodies at the indicated concentration or with anti-CD3/CD28 coated beads. **(C)** The mean fluorescence intensity (MFI) of CD25 in HCs (n=4) and patients (n=8) analyzed under the same conditions. (**A-C**) Data indicate mean with SD. P values were determined in a Mann-Whitney test. NS, not-significant.

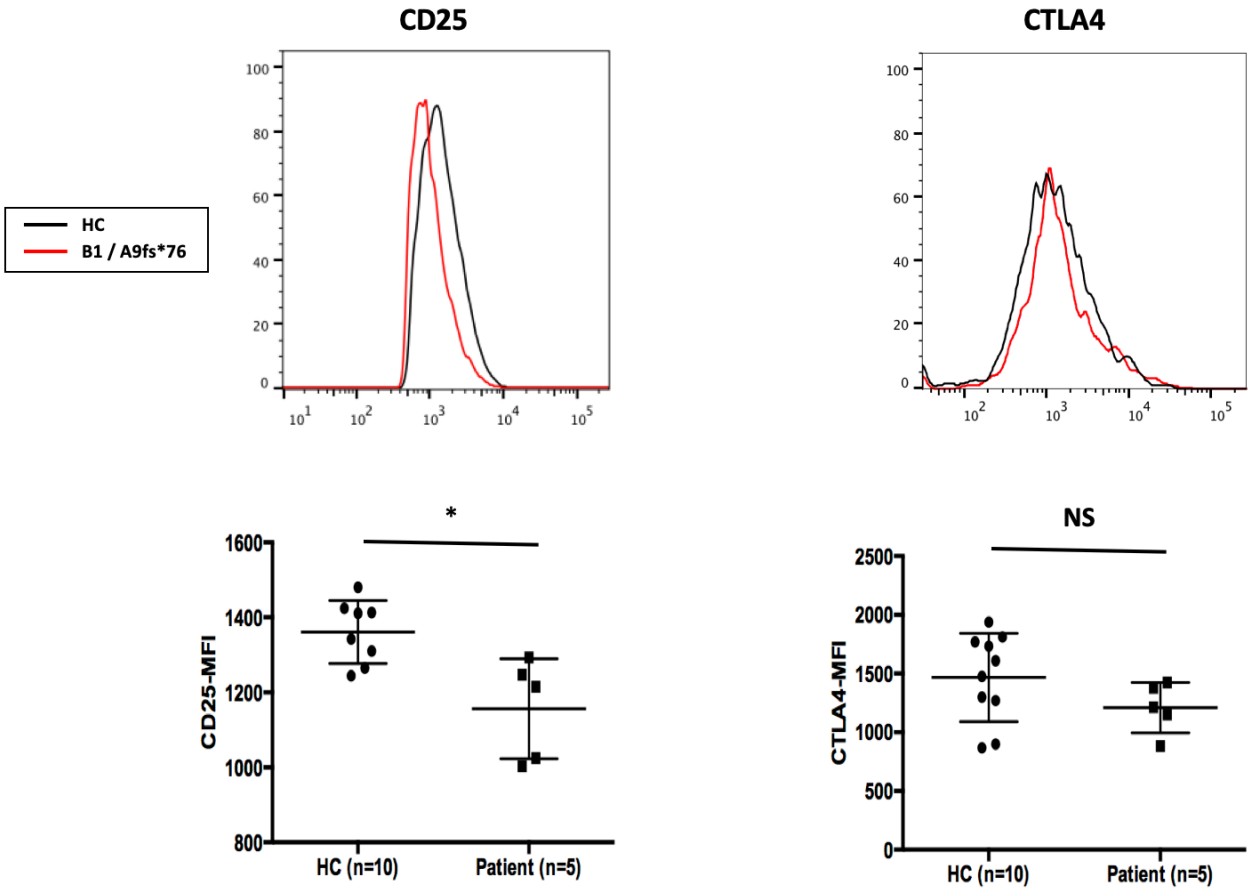

Supplementary Figure 11. CD25 and CTLA-4 expression in regulatory T cells

Top: representative histograms of CD25 and CTLA-4 expression in $CD4^{+}CD25^{+}CD127^{low}$ T_{reg} cells from an HC (black) and patient B1 (p.A9fs*76 mutation) (red). Bottom: mean fluorescence intensity (MFI) of the respective T_{reg} cell markers in HCs (n=10) and patients (n=5). The plots correspond to the mean ± SD, and each dot corresponds to an individual. Data indicate mean with SD. Two-tailed p values were determined in a Mann-Whitney test (CD25 p = 0.0109). *P ≤ 0.05; NS, non-significant.

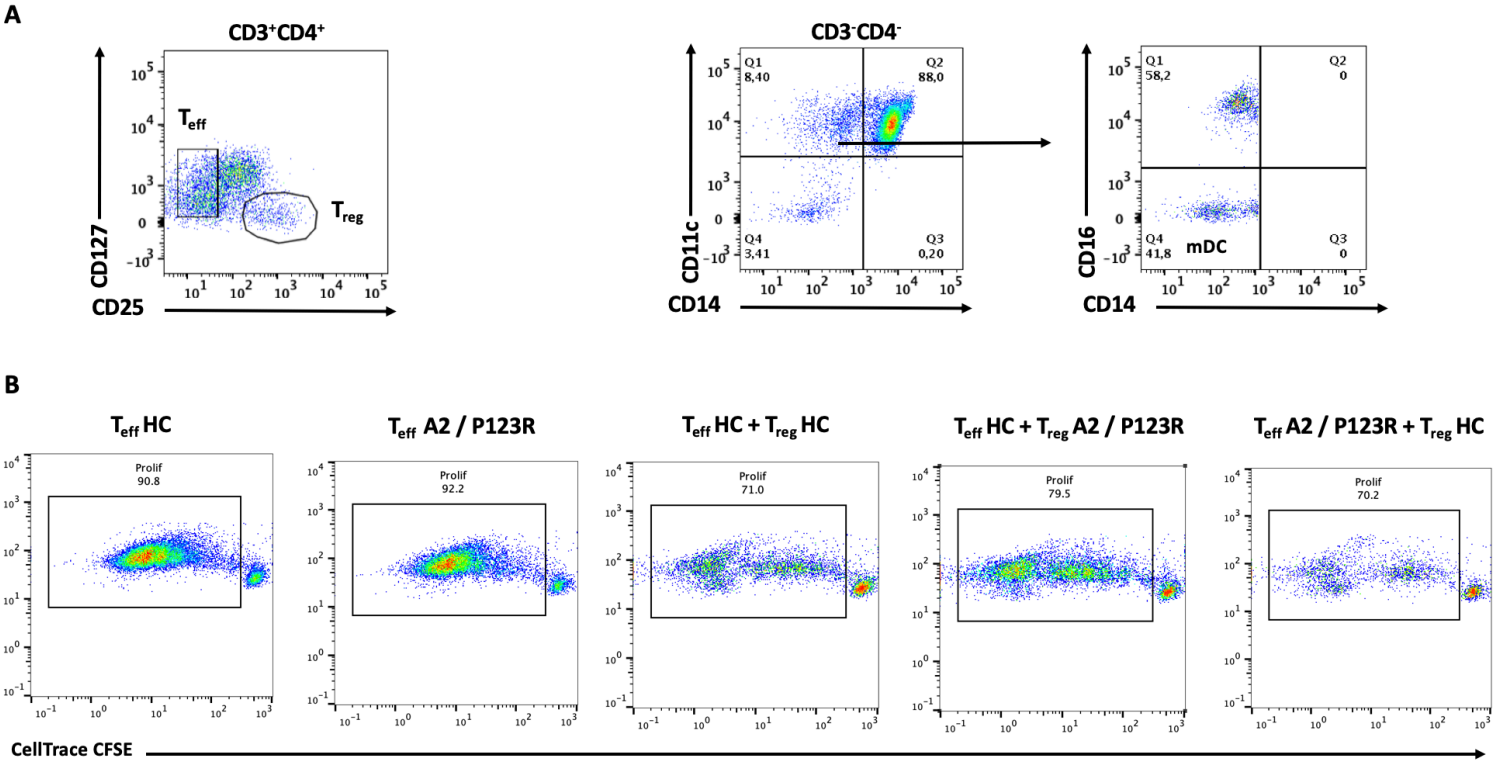

Supplementary Figure 12. Gating strategy for suppressive assay of T_{reg} cells

(A) Gating strategy for sorting effector T cells (T_{eff} CD3+CD4+CD127+CD25-), regulatory T cells (T_{reg} CD3+CD4+CD127-CD25+) (left), and dendritic cells (DCs $CD3^{-}CD14^{-}CD16^{-}CD11c^{+}$) (right).

(B) Representative flow cytometry analysis showing the proliferation of T_{eff}-HC alone, Teff-patient A2 (p.P123R mutation) alone, T_{eff}-HC/T_{reg}-HC, T_{eff}-HC/T_{reg}-patient A2, and T_{eff}-patient/T_{reg}-HC.

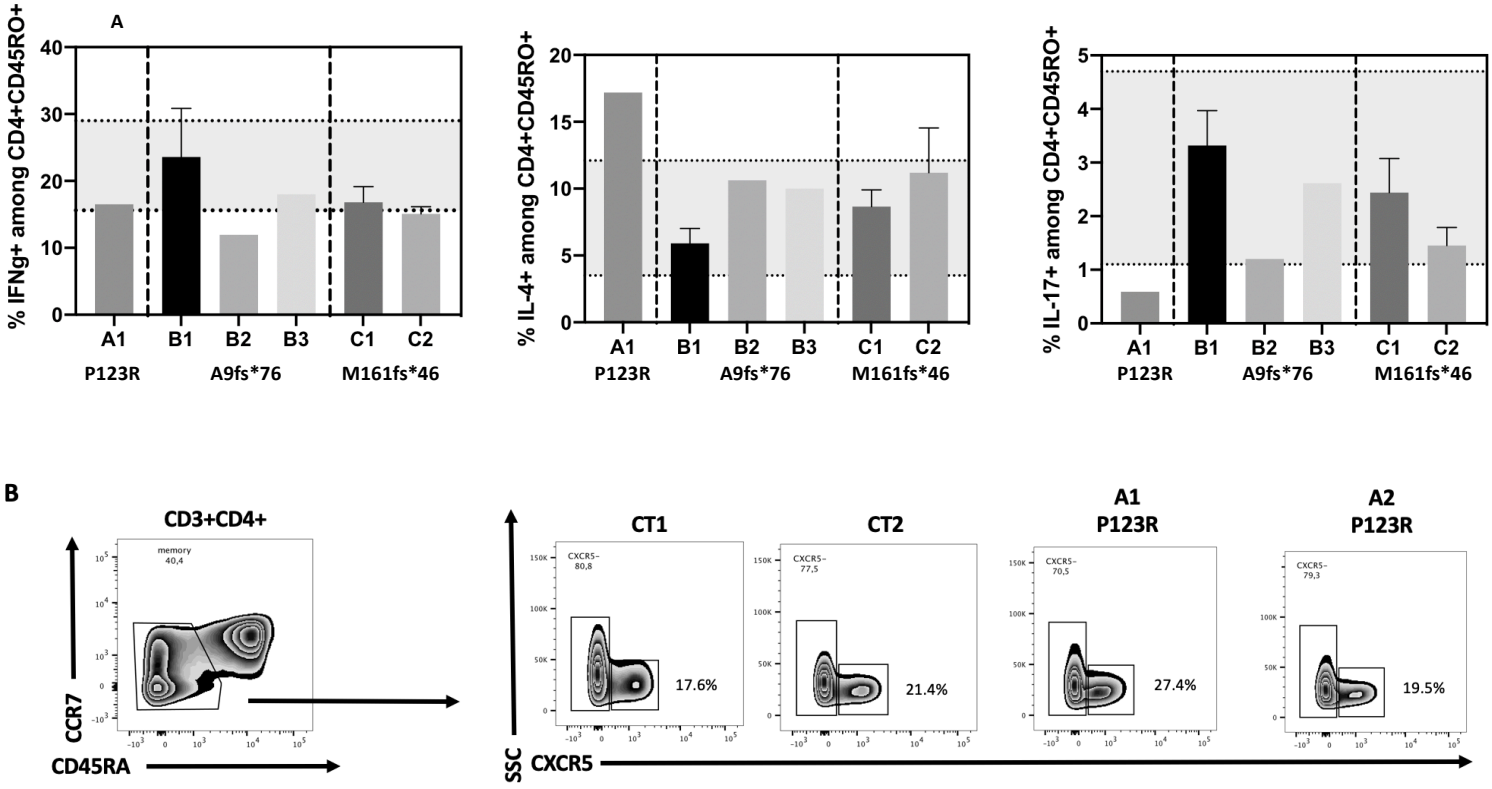

Supplementary Figure 13. CD4⁺ T-helper cell differentiation

(A) Distributions of Th1, Th2 and Th17 subsets (as a percentage of total $CD4^+CD45RO^+$ memory T cells) among patients and asymptomatic carriers with *SOCS1* mutations. Peripheral blood mononuclear cells from patients (A1, B1, B2, and C1), asymptomatic carriers (C2, B3) and HCs were stimulated *ex vivo* with phorbol myristate acetate and ionomycin and then stained for intracellular IL-4, IL-17A and IFN-γ. The gray shaded area represents the median [5^{th} and 95^{th} percentiles] from 40 HCs. Data are presented as median with SD between measurements done at 2 different time points. **(B)** Flow cytometry analysis of circulating follicular helper T (T_{FH}) cells ($CD4^+CXCR5^+$) gated from total memory $CD4^+$ T cells (left) in healthy controls (CTs) and patients (A1 and A2 with p.P123R mutation).

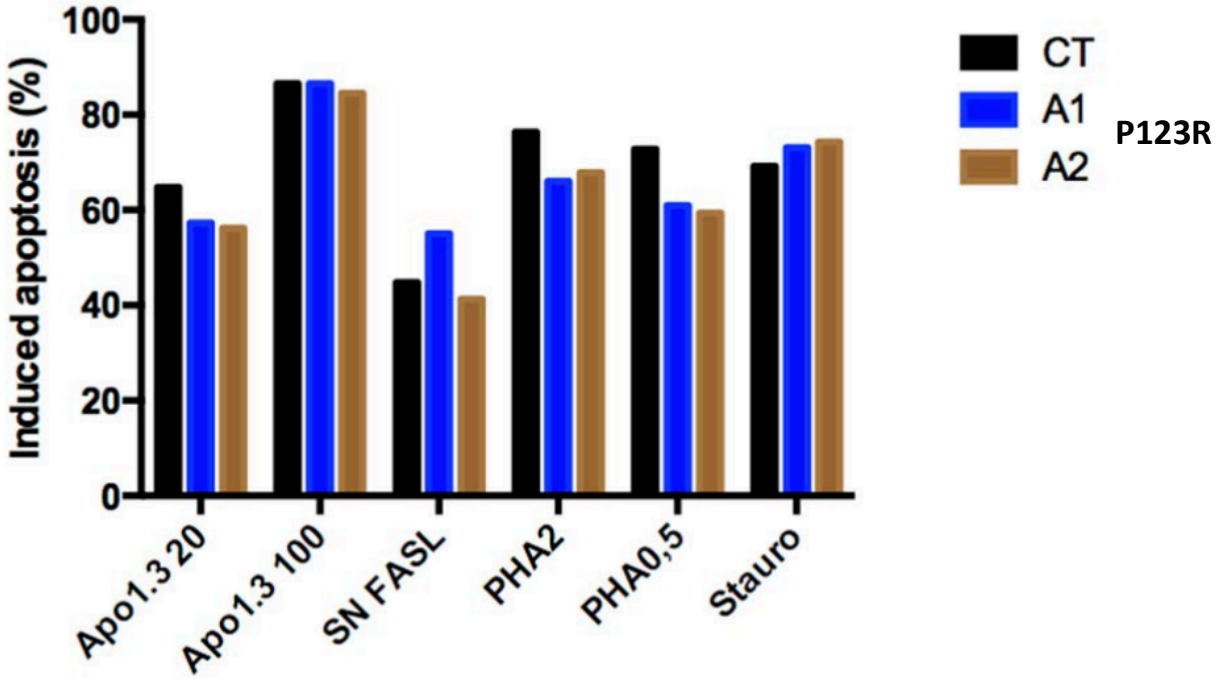

Supplementary Figure 14. T cell apoptosis assay.

T cell blasts ($CD3^+$) apoptosis induced by FAS agonist (APO1.3 20 and 100ng/ml), FAS-ligand (SN FASL), phytohaemagglutinin (PHA 0.5 or 2microg/ml) and Staurosporin (Stauro) in healthy controls (CT) and patients (A1 and A2 with p.P123R mutation). Experiment performed once.

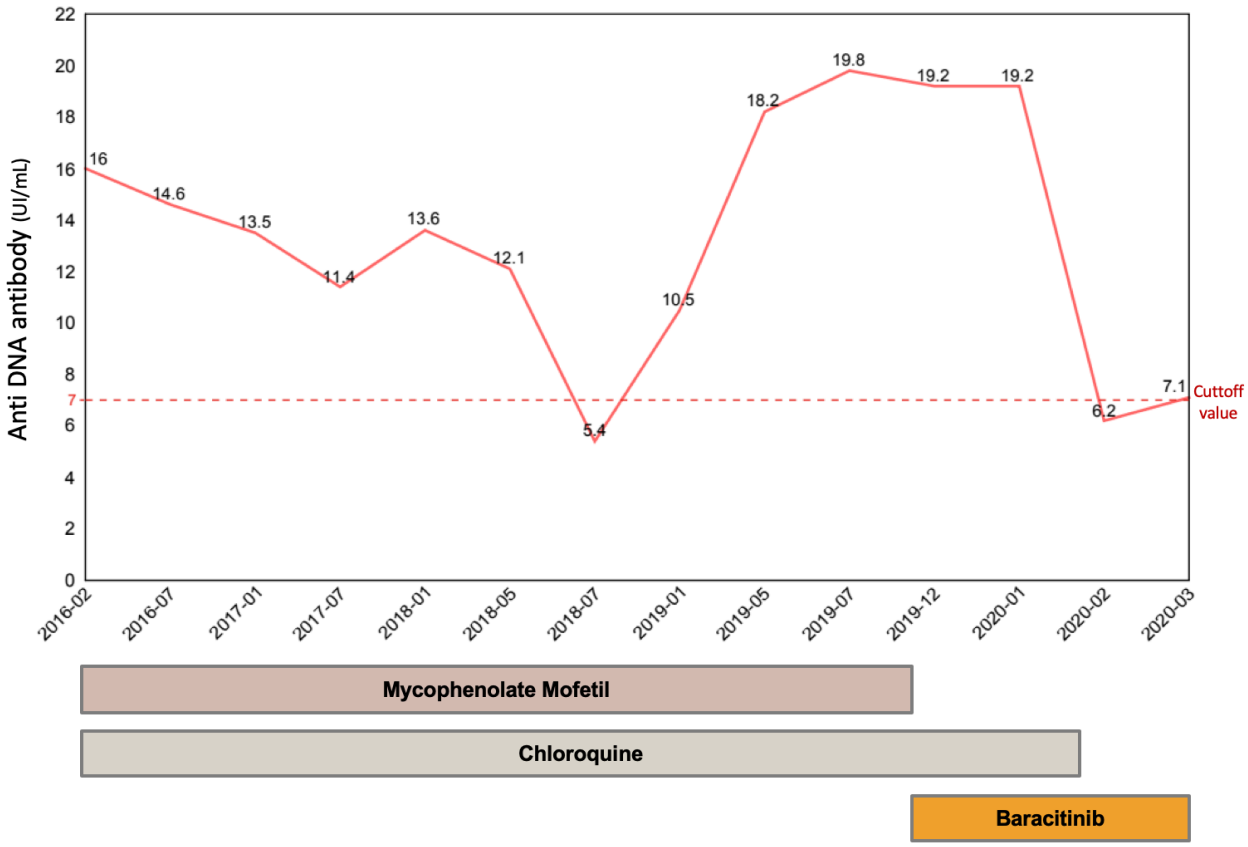

Supplementary Figure 15. Level of anti-DNA antibody

Evolution of anti-DNA antibodies level of patient E1 (p.Y154H mutation) measured by Farr assay (from February 2016 to march 2020) as a function of the treatments received.